



## Role of plasma inhomogeneities in the generation of broadband waves in the polar ionosphere

Alexander Chernyshov<sup>\*(1)(2)</sup>, Andres Spicher<sup>(3)</sup>, Askar Ilyasov<sup>(1)(2)</sup>, Wojciech Miloch<sup>(3)</sup> and Mikhail Mogilevsky<sup>(1)</sup>

(1) Space Research Institute of the Russian Academy of Sciences, 84/32 Profsoyuznaya Street, 117997, Moscow, Russia

(2) West Department of Pushkov Institute of Terrestrial Magnetism, Ionosphere and Radio Wave Propagation, RAS, 236017, Pobedy av. 41, Kaliningrad, Russia

(3) Department of Physics, University of Oslo, Box 1048 Blindern, N-0316 Oslo, Norway

### Abstract

It is shown that plasma instability associated with an inhomogeneous energy density distribution can lead to the excitation of electrostatic ion-cyclotron and oblique ion-acoustic waves generated in the presence of inhomogeneous electric field and shear in the ion parallel drift velocities. Microprocesses associated with plasma inhomogeneities are studied on the basis of data from satellite and sounding rocket. By numerical stability analysis it is demonstrated that inhomogeneous-energy-density-driven instability (IEDDI) can be a mechanism for the excitation of small-scale plasma inhomogeneities. The Local Intermittency Measure (LIM) method also applied the rocket data to analyze irregular structures of the electric field during rocket flight in the cusp. A qualitative agreement between high values of the growth rates of the IEDDI and the regions with enhanced LIM is observed. This suggests that IEDDI is connected to turbulent non-gaussian processes.

### 1 Introduction

The polar ionosphere is a very complex area of precipitating, mirrored and upwelling ions and electrons with the presence of magnetic and electric field perturbations and turbulence, which attest the importance of the high-latitude region in the transport of energy in magnetosphere-ionosphere coupling. Therefore, the study of microprocesses in the high-latitude region of the ionosphere and magnetosphere has been actively performing over the past few decades. The broadband low-frequency turbulence is one example of such processes. This turbulence consists of the broadband fluctuations of electric and magnetic fields that are repeatedly observed by satellites and sounding rockets. In spite of the considerable progress in this area, many questions remain to be answered. These issues are related to the sources of the broadband electrostatic noise and wave modes that participate in generation of this noise. The most appropriate candidates are oblique ion-acoustic and electrostatic ion-cyclotron waves.

Broadband electrostatic perturbations are detected in the presence of gradients of electric and magnetic fields, that is, in essentially inhomogeneous plasma configurations. The

theory of waves, generated by inhomogeneous distribution of energy density (IEDDI - inhomogeneous energy-density-driven instability), was initially developed in the articles [1, 2]. This instability mechanism does not explicitly depend on any specific shear in the  $E \times B$  equilibrium velocity. Instead, it requires neighboring regions in space with different signs of wave energy density which may be generated by a localized flow profile. If a coupling between these two regions is possible such that the energy can flow from the region with negative wave energy density to the adjacent region with positive wave energy, the instability can grow while the total energy remains constant as required by the energy conservation principle. Subsequently it was suggested that this instability leads to formation of the broadband electrostatic turbulence [3, 4]. Also, the IEDDI is believed to take a principal part for ion energization and up-flow from the ionosphere into the magnetosphere both in the cusp and auroral region [2]. In this paper, we consider in detail the IEDDI and generation of broadband perturbations in various high-latitude parts of the ionosphere. To do this, we use FAST satellite data as well as the results of the rocket experiment to study the cusp ionosphere.

### 2 Governing equations

Nonlocal instabilities in a plasma driven by inhomogeneities of field-aligned current and electric field are considered. The theory of these instabilities is described in detail in [2]. Uniform magnetic field is directed along the  $z$  axis, nonuniform electric field is along the  $x$  axis. Plasma is inhomogeneous in the  $x$  direction as well. Unknown function  $\psi$  is normalized potential of electric field.

$$\frac{d^2\psi}{d\xi^2} + \kappa^2(\xi)\psi = 0 \quad (1)$$

$$\kappa^2(\xi) = -2 \frac{1 + \sum_n \Gamma(b) F_{ni}(\xi) + \tau(1 + F_{0e})}{\sum_n \Gamma'(b) F_{ni}(\xi)} \quad (2)$$

here  $F_{n\alpha} = A_{n\alpha}(x) - B_{n\alpha}(x)$  and

$$A_{n\alpha}(x) = \frac{(\omega_{1\alpha} + \omega_{2\alpha} - \omega_{* \alpha})}{\sqrt{2}|k_z|v_{i\alpha}} Z\left(\frac{\omega_{1\alpha} + \omega_{2\alpha} - n\Omega_{\alpha}}{\sqrt{2}|k_z|v_{i\alpha}}\right) \quad (3)$$

$$B_{n\alpha} = \frac{\omega_{3\alpha}}{2|k_z|v_{t\alpha}} Z' \left( \frac{\omega_{1\alpha} + \omega_{2\alpha} - n\Omega_\alpha}{\sqrt{2}|k_z|v_{t\alpha}} \right) \quad (4)$$

where  $\xi = x/\rho_i$ ,  $b = (k_y\rho_i)^2/2$ ,  $\tau = T_i/T_e$  is the ratio of ion temperature to electron temperature,  $v_{t\alpha}$  is the thermal velocity of particles of species  $\alpha$ ,  $\Omega_\alpha$  is the gyrofrequency of particles of species  $\alpha$ ,  $\omega_{1\alpha} = \omega - k_y V_E - k_z V_{d\alpha}$  is the Doppler shifted frequency,  $V_E(\xi)$  is the velocity of  $E \times B$  drift,  $\omega_{2\alpha} = k_y V_E'' \rho_\alpha^2/2$ ,  $\omega_{3\alpha} = k_y V_{d\alpha}' \rho_\alpha$ ,  $V_{d\alpha}$  is the field-aligned current of species  $\alpha$ ,  $\omega_\alpha^* = k_y \Omega_\alpha \rho_\alpha \varepsilon_n$ ,  $\varepsilon_n = (\rho_\alpha n_0(\xi))/(\frac{dn_0(\xi)}{d\xi})$ ,  $\Gamma_n(b) = \exp(-b)I_n$ ,  $I_n$  are the modified Bessel functions,  $\Gamma_n' = \frac{d\Gamma_n}{db}$ ,  $Z$  is the plasma dispersion function,  $Z'$  is the derivative of the Z-function.

The study of the instability reduces to the eigenvalue problem. One has to find  $\omega = \omega_r + i\gamma$  for which solution of eigenvalue equation (1) exists and the growth rate  $\gamma$  is positive. The solution must fade when coordinate  $\xi$  tends to infinity, i.e.,  $\psi(\pm\infty) = 0$ . Note that the eigenvalue condition for the ion-acoustic mode is the same as that for ion-cyclotron mode. Since the velocity shear effect is represented by the term proportional to  $k_y V_E$  in the dispersion relation (1), only the oblique ion-acoustic mode can be affected by transverse velocity shear. Thus, we hereafter consider only the oblique ion-acoustic modes.

### 3 Numerical aspects and modeling results

In order to solve the eigenvalue problem, the shooting method is used. The interval considered for stability analysis is divided into layers, where  $\kappa^2(\xi)$  is assumed to be constant. Thus,  $\psi$  is the sum of two exponents in each layer, i.e.  $\psi_j(\xi) = B_j \exp(i\kappa_j \xi) + \tilde{B}_j \exp(-i\kappa_j \xi)$ , where  $j$  is the number of layer, and  $B_j$  and  $\tilde{B}_j$  are constant. For the first and the last layers,  $\psi$  contains only one exponential and the sign of  $\kappa_j$  corresponds to the boundary condition, i.e. the single term  $\exp(i\kappa_j \xi)$  should become zero at infinity. It is also necessary that the solution obtained is continuously differentiable on the whole  $x$  axis. This matching condition is satisfied by linear algebraic expressions containing coefficients before the exponentials, as shown in more detail in [3]. First, let us consider the possibility of exciting electrostatic ion-cyclotron waves in the polar ionosphere using satellite data. The results of modeling that take into account only the electric field are demonstrated in Fig.1. In this case, the electric field configuration was taken from the FAST satellite data, which are presented in Fig. 2. The background plasma parameters in the numerical calculation were chosen as follows:  $t = 0.5$ ,  $u = 0.1$ ,  $V_d = 0.9v_{te}$ ,  $r_i = 20$  m. The instability regions are localized along two curves similar to parabolas with a vertex at the cyclotron resonance, and near small  $b$  and  $w_r \sim 0.9W_i$ . The grid step for the shooting method was 0.002 for  $w_r$  and 0.003 for  $b$ . Black shows the regions of  $\gamma$  values greater than 0.002. One can see that the growth rate of IEDDI increases with parameter  $b$  increasing. In other words, the growth rate at small  $b$  is close to zero. It can be explained as follows: when electrons get in Landau resonance with

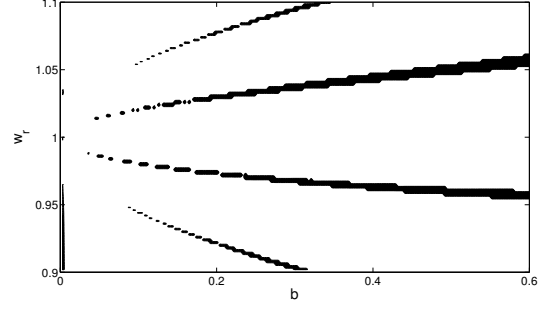


**Figure 1.** The growth rate of the IEDDI depending on parameter  $b$  and real part of wave frequency. Only inhomogeneous electric field observed by FAST is included in the simulation.

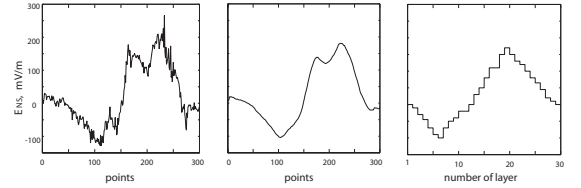
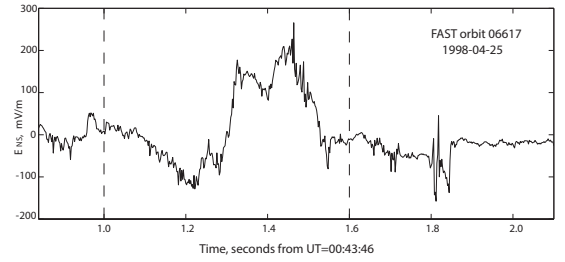


**Figure 2.** Profile of inhomogeneous electric field measured by the FAST satellite

the wave field near the ion gyrofrequency, the cyclotron damping becomes significant and instability is damped. It is shown that the IEDDI is generated in a wide range of real wave frequencies  $\omega_r$  and transverse wave numbers  $k_y$ . This can manifest as broadband spectrum in satellite observations. Let us now consider the possibility of excitation of oblique ion-acoustic modes by the IEDDI in the high-latitude region. Simulation results for ion acoustic branch with taking into account gradients of field-aligned velocity are shown in Fig. 3. The contour diagrams of instability increment  $\gamma$  are presented in coordinates  $w_r$  and  $b$  to show the solution dependence on the basic parameters (dimensionless frequency and wave number) of the disturbance. Gradation of  $\gamma$  displayed in gray in the diagrams reflects its value: the darker color corresponds to the larger value  $\gamma$ . In the nonlocal formulation, the oblique ion acoustic waves are not excited in the domain where  $\omega_r > 0.13\Omega_i$ . As in the case of ion cyclotron waves, the growth rate of instability increases with parameter  $b$  [3] but the difference in the growth rate of ion-acoustic waves for small and large values of  $b$  is less pronounced. It is interesting to note that the

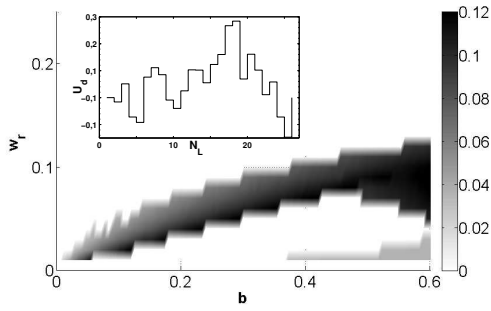


**Figure 3.** Simulation results for the case in which only the inhomogeneous ion parallel velocity is considered. The values of growth rate of the instability are indicated by shades in gray (scale on the right). In the insert, the inhomogeneous configuration of the electron parallel velocity is shown approximated by a piecewise constant function, where  $N_L$  is the number of layers, and  $U_d$  is the electron parallel velocity normalized over the thermal velocity

ion acoustic waves are excited in a wide range of frequencies and there is no clear maximum at any frequency. Flow shears are very common in the polar ionosphere in connection with discrete auroral forms, and so can be important for the development of ionospheric irregularities and turbulence. One particular cusp phenomenon associated with sheared plasma flows and density irregularities is the Reverse Flow Event (RFE) [5], which is defined as a 100-200 km wide quasistatic east-west elongated channel where the flow is in the opposite direction with respect to the background flow. It is found an immediate response in enhanced HF backscatter power data associated with several RFEs, implying a rapid development of decameter-scale irregularities [5]. One of the possible mechanisms to produce small-scale structures is the IEDDI. It was suggested that the IEDDI could influence cusp and cleft dynamics [2], however, experimental and numerical works devoted to this question are still sparse. Thus, in order to investigate the role of the IEDDI in the cusp ionosphere, we performed numerical stability analysis of the IEDD instability using data from the Investigation of Cusp Irregularities 3 (ICI-3) rocket. The ICI-3 sounding rocket was launched from Ny-Alesund at 07:21:31UT on December 3, 2011 [6]. ICI-3 rocket intersected a RFE. The various measurements made by the ICI-3 sounding rocket with respect to time of flight between 150 s and 500 s are shown in detail in Fig.4. The corresponding altitudes are  $h = 236.8$  km and  $h = 202.8$  km. The ICI-3 rocket intersected the RFE between about  $t = 250$  s and  $t = 380$  s of the flight [6].

In order to study the correlation between generation of the IEDDI and irregular structures in the electric field, we use the Local Intermittency Measure (LIM), as the degree of irregularity dependences on scales. We performed a LIM analysis using wavelet transforms [7]. The LIM is de-

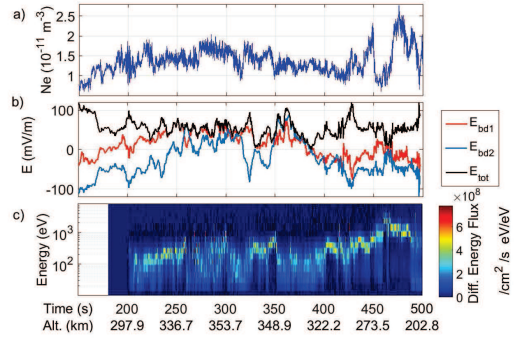


**Figure 4.** ICI-3 sounding rocket measurements with respect to time of flight and altitude: a) Electron density. b) Components (red and blue) and magnitude (black) of the electric field. c) Electron particle precipitation flux at  $0 - 30^\circ$  pitch angle.

defined as  $LIM(s, t) \equiv |W_s(t)|^2 / \langle |W_s(t)|^2 \rangle_t$ , where  $\langle \dots \rangle_t$  corresponds to the averaging over time, and  $W_s(t)$  are the wavelet coefficients for the electric field at scales  $s$  and time  $t$  [7]. As  $\langle |W_s(t)|^2 \rangle_t$  is equivalent to the Fourier spectrum, the condition  $LIM = 1$  means that each part of the signal has the same energy spectrum as the Fourier spectrum and that the signal does not exhibit intermittency, which is characterized by the degree of non-uniformity of the wavelet power. On the other hand, values of the LIM greater than one indicate intermittency.

For each of the 20 seconds interval, the LIM was calculated for the electric field  $E_{LIM}(t) = E(t) - E(t_0)$ , where  $t_0$  is the time in the beginning of each intervals (this was done to match the normalization used for the numerical analysis). For comparison with the growth rates of the IEDDI and to obtain a rough estimate of the LIM in each interval, the median of the LIM at each scale was calculated for each interval. The median LIM at each scale is plotted in Fig. 5 e) and f) with respect to time and frequency, which ranges from 0.1 Hz to 10 Hz due to restrictions associated with the cone of influence at lower frequency and the electric field resolution. Again, the values shown at each time correspond to the median LIM obtained for the 20 seconds intervals following that time. Several regions with enhancements in the LIM over many frequency scales can be observed, in particular at about 210 s, 250 s, 270 s, 350 and at the end of the flight, implying the presence of the enhanced "local activity" of the electric field in those intervals for several frequencies (or scales). By comparing Fig. 5 c) and d) with Fig.5 e) and f), one can observe a qualitative agreement between those regions with enhanced growth rate values and those with enhanced LIM. In particular, all the intervals with large growth rate relate to enhancements in the LIM, and thus in electric field inhomogeneities. In other words, the IEDDI exists in turbulent intermittent (or non Gaussian) process in the cusp. It should however be noted that the presence of LIM does not necessary always imply that IEDDI is active, as visible for example at about 410 s. Perhaps, in this case, there are other plasma instabilities

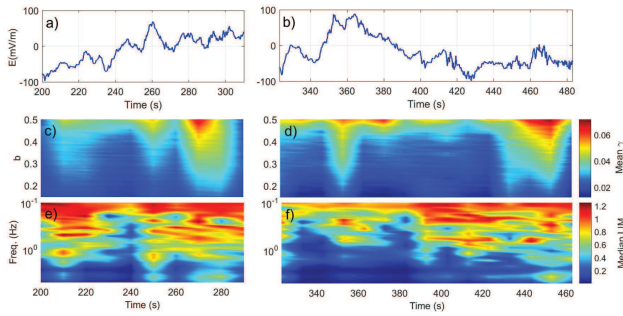


**Figure 5.** a) and b) Electric field data measured by ICI-3. c) and d) Growth rate of the IEEDI normalized by the oxygen ion gyrofrequency depending on the parameter  $b$  averaged over the real part of the wave frequency  $\omega_r$  for intervals of 20 s with 10 seconds overlap. e) and f) Median of the LIM for the same intervals as in panel c) and d).

that are responsible for irregular processes.

## 4 Conclusions

In this study, the most probable physical mechanism of broadband electrostatic turbulence accompanying Alfvén turbulence in the higher-frequency region of the spectrum (up to 1 kHz) is proposed. The mechanism is based on the theory of generation of broadband waves by inhomogeneous transverse quasistatic electric fields and a shear in the field-aligned particle velocity in the high-latitude ionosphere. It is shown that the non-uniform electric fields of Alfvén turbulence can destabilize the electrostatic ion-cyclotron waves, which are obtained as unstable solutions of the nonlocal dispersion equation and whose properties differ significantly from the properties of classical ion-cyclotron waves. It has also been demonstrated that the oblique ion-acoustic modes can be excited because of the shear in the field-aligned velocity of the ions. Moreover, for waves of ion-acoustic type, the IEEDI provides a broadband spectrum in the frequency range on the order of 0.1 of the ion gyrofrequency. For waves of ion cyclotron type, the instability is excited in a wide range of frequencies near the ion gyrofrequency without a clearly expressed maximum. Consequently, the spectrum of IEEDI waves contains a lot of eigen frequencies and wavelengths that provide a broadband spectrum, which is in good agreement with the known observational data. In other words, electrostatic broadband turbulence can be identified as a kind of electrostatic ion cyclotron or/and oblique ion acoustic waves excited by a nonuniform wave energy density distribution.

We have shown that the IEEDI is active in the high-latitude ionosphere using rocket data, both on the sides and in the center of the RFE. This supports the idea that microscale irregularities in cusp flow events (such as RFEs) are connected with the action of this instability. A secondary generation of microscale inhomogeneities by the IEEDI on the background evolution of a primary instability such as Kelvin-Helmholtz instability might thus be well suited

for describing RFE irregularities, where the electric field is quite inhomogeneous. We also showed that the IEEDI growth rate is facilitated in the presence of enhanced inhomogeneities in the electric field, and that it is strongly affected by field-aligned velocities. This was supported by a LIM analysis, which shows that large growth rate of the IEEDI corresponded to high values of LIM at different scales, indicating that the IEEDI is connected with the creation of turbulent non-gaussian processes.

## 5 Acknowledgements

We thank L.B.N. Clausen, J.I. Moen, Y. Saito, I.V. Golovchanskaya and B.V. Kozelov for fruitful discussions. The work of A.C. and A.I. was supported by the Russian Science Foundation (grant 17-77-20009). Authors acknowledge the Norwegian Center for International Cooperation in Education - SIU (UTF-2016-short-term/10026).

## References

- [1] G. Ganguli, Y. C. Lee, and P. G. Palmadesso (1985), Electrostatic ion-cyclotron instability caused by a nonuniform electric field perpendicular to the external magnetic field, *Physics of Fluids*, 28, 761–763, doi: 10.1063/1.865096.
- [2] G. Ganguli, M. J. Keskinen, H. Romero, R. Heelis, T. Moore, and C. Pollock (1994), Coupling of micro-processes and macroprocesses due to velocity shear: An application to the low-altitude ionosphere, *J. Geophys. Res.*, 99, 8873–8889, doi:10.1029/93JA03181.
- [3] A. A. Ilyasov, A. A. Chernyshov, M. M. Mogilevsky, I. V. Golovchanskaya, and B. V. Kozelov (2015), Inhomogeneities of plasma density and electric field as sources of electrostatic turbulence in the auroral region, *Phys. Plasmas*, 22(3), 032906, doi:10.1063/1.4916125.
- [4] A. A. Chernyshov, A. Ilyasov, M. Mogilevsky, I. Golovchanskaya, and B. Kozelov (2015), Influence of inhomogeneities of the plasma density and electric field on the generation of electrostatic noise in the auroral zone, *Plasma Phys. Rep.*, 41(3), 254–261, doi: 10.1134/S1063780X15030010.
- [5] Y. Rinne, J. Moen, K. Oksavik, and H. C. Carlson (2007), Reversed flow events in the winter cusp ionosphere observed by the European incoherent scatter (EISCAT) Svalbard radar, *J. Geophys. Res.*, 112(A10), doi:10.1029/2007JA012366.
- [6] A. Spicher, A. A. Ilyasov, W. J. Miloch, A. A. Chernyshov, L. B. N. Clausen, J. I. Moen, T. Abe, and Y. Saito (2016), Reverse flow events and small-scale effects in the cusp ionosphere, *J. Geophys. Res.*, 121, 10, doi:10.1002/2016JA022999.
- [7] M. Farge (1992), Wavelet transforms and their applications to turbulence, *Ann. Rev. Fluid Mech.*, 24(1), 395–458, doi:10.1146/annurev.fl.24.010192.002143.